

Depinning and creep motion in glass states of flux lines

Meng-Bo Luo^{†,‡} and Xiao Hu[†]

[†]Computational Materials Science Center, National Institute for Materials Science, Tsukuba 305-0047, Japan

[‡]Department of Physics, Zhejiang University, Hangzhou 310027, China

(Dated: September 4, 2018)

Using dynamical computer simulation we have investigated vortex matters in glass states. A genuine continuous depinning transition is observed at zero temperature, which also governs the low-temperature creep motion. With the notion of scaling, we evaluate in high accuracy critical exponents and scaling functions; we observe a non-Arrhenius creep motion for weak collective pinning where Bragg glass (BrG) is stabilized at equilibrium, while for strong pinning the well-known Arrhenius law is recovered. In both cases, a sharp crossover takes place between depinning and creep at low temperatures. The possible relation between the present results and a recent experimental observation of a second-order like phase boundary inside the BrG phase is discussed.

PACS numbers:

Introduction – Depending on the strength of the random pinning force, the equilibrium state of the flux lines at low enough temperature can be either Bragg glass (BrG) [1, 2], where quasi long-range lattice order still survives, or vortex glass (VG) [3] as random as the liquid phase. The competition between the vortex repulsion and the random pin potential builds up a highly nontrivial energy landscape, which manifests itself drastically in dynamics, e.g. vortex motion under current driving. Since the proposal of collective pinning theory of vortex lines by Larkin and Ovchinnikov [4], theoretical understanding for the nonlinear dynamics response has been advanced [1, 5, 6, 7, 8]. The functional renormalization group (FRG) has also been formulated [9]. For recent review articles see [10, 11, 12].

The current-driven flux lines compose a unique system of $D = 3$ dimensions in the internal space, equal to the dimension $d = 3$ of the space where the system is embedded, and $N = 2$ components of displacement vector. A full FRG treatment is still not available for $N > 1$. We try to address the issue by computer simulations, with the hope that useful insights complimentary to the previous works can be provided. It is recalled that computer simulations for a domain wall in a plane with $N = 1$, $D = 1$ and $d = 2$ were reported recently [13].

On the other hand, a new experimental finding of a second-order like phase boundary in $H - T$ phase diagram was reported very recently, which intersects the first-order phase boundary associated with the melting transition of the BrG [14]. It certainly renews interests on corresponding variations in dynamical properties inside the BrG phase; the new phase transition was discussed in terms of replica-symmetry breaking [15], which is perhaps best captured by dynamical responses.

The main results of the present work are summarized as follows: Based on the simulation results, we have derived a scaling relation among the velocity, force and temperature with two universal exponents for vortex motions around the zero-temperature depinning force. From the exponents and the scaling curve, the Arrhenius law for the creep motion with a linearly suppressed energy

barrier appears for strong pinning strength. A non-Arrhenius type creep motion is observed at weak collective pinning for which the equilibrium state is a BrG. A sharp crossover between the depinning and creep motion is also observed.

Model and simulation details – We consider a superconductor of layered structure with magnetic field perpendicular to the layers. The model system is a stack of superconducting planes of thickness d with interlayer space s . Each plane contains N_v pancake vortices (PV) and N_p quenched pins. The overdamped equation of motion of the i th pancake at position \mathbf{r}_i is [16, 17, 18, 19, 20]

$$\eta \dot{\mathbf{r}}_i = - \sum_{j \neq i} \nabla_i U^{VV}(\mathbf{r}_{ij}) - \sum_p \nabla_i U^{VP}(\mathbf{r}_{ip}) + \mathbf{F}_L + \mathbf{F}_{th}. \quad (1)$$

Here η is the viscosity coefficient. The vortex-vortex interaction contains two parts: an intraplane PV-PV pairwise repulsion given by the modified Bessel function $U^{VV}(\rho_{ij}, z_{ij} = 0) = d\epsilon_0 K_0(\rho_{ij}/\lambda_{ab})$, and an interplane attraction between PVs in adjacent layers given by $U^{VV}(\rho_{ij}, z_{ij} = s) = (s\epsilon_0/\pi)[1 + \ln(\lambda_{ab}/s)][(\rho_{ij}/2r_g)^2 - 1]$ for $\rho_{ij} \leq 2r_g$ and $U^{VV}(\rho_{ij}, z_{ij} = s) = (s\epsilon_0/\pi)[1 + \ln(\lambda_{ab}/s)][\rho_{ij}/r_g - 2]$ otherwise, where $\epsilon_0 = \phi_0^2/2\pi\mu_0\lambda_{ab}^2$ with λ_{ab} the in-plane magnetic penetration depth, $r_g = \gamma\xi_{ab}$ with ξ_{ab} the in-plane coherence length and γ the anisotropy [16, 19]. Here, ρ_{ij} is the in-plane component of position vector \mathbf{r}_{ij} between i th and j th PVs and z_{ij} is that along layer normal. The pinning potential is given by $U^{VP}(\rho_{ip}) = -\alpha A_p \exp[-(\rho_{ip}/R_p)^2]$, where $A_p = (\epsilon_0 d/4) \ln[1 + (R_p^2/2\xi_{ab}^2)]$ and α is the dimensionless pinning strength. Finally, \mathbf{F}_L is the uniform Lorentz force, and \mathbf{F}_{th} is the thermal noise force with zero mean and a correlator $\langle F_{th}^\alpha(z, t) F_{th}^\beta(z', t') \rangle = 2\eta T \delta^{\alpha\beta} \delta(z - z') \delta(t - t')$ with $\alpha, \beta = x, y$. We consider a material similar to $\text{Bi}_2\text{Sr}_2\text{CaCu}_2\text{O}_8$ with $\kappa = \lambda_{ab}/\xi_{ab} = 90$, $\gamma = 100$, and $d = 2.83 \times 10^{-3} \lambda_{ab}$, $s = 8.33 \times 10^{-3} \lambda_{ab}$, with $R_p = 0.22 \lambda_{ab}$ [19]. Below the units for length, energy, temperature, force and time are taken as λ_{ab} , $d\epsilon_0$, $d\epsilon_0/k_B$, $d\epsilon_0/\lambda_{ab}$, and $\eta\lambda_{ab}^2/d\epsilon_0$. Pinning strength is sup-

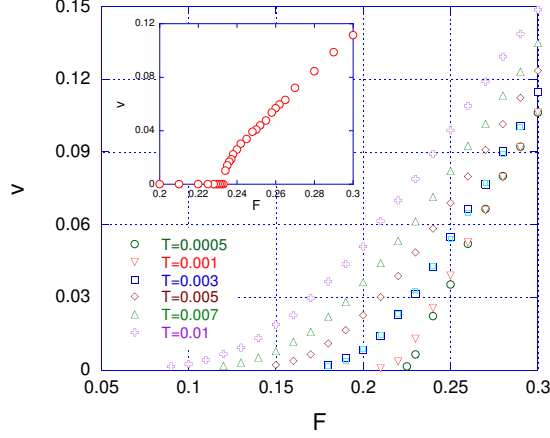


FIG. 1: $v - F$ characteristics for $\alpha = 0.2$. Data for $T = 0.003$ obtained for $L_{xy} = 40\lambda_{ab}$ are also included (light-blue squares). Inset: data for zero temperature. Error bars are smaller than the size of symbols.

posed to be uniform. Periodic boundary conditions are put in all the three directions. The results shown below are for $N_v = 180$, $N_p = 900$, $N_z = 20$, $L_{xy} = 30$. The magnetic field is roughly $B \simeq 100G$ if we take $\lambda_{ab} = 2000\text{\AA}$ [21]. The equation is integrated by the 2nd order Rugen-Kutter algorithm with $\Delta t = 0.002 \sim 0.01$. All data presented below are the average over 10 samples with different randomly distributed pins. Fixing the magnetic field, we have performed simulations for $L_{xy} = 20$ and 40 , and make sure that finite-size effects are negligible to the main, universal results. For pinning strength, we choose $\alpha = 0.2$ and $\alpha = 0.05$, for which the maximal curvatures of the pinning potential are 4.87 and 1.22 , above and below the tilt modulus of the flux lines $\bar{C} \simeq 1.47$; they are therefore expected to fall into the strong and weak collective pinning regimes respectively [22, 23].

Strong pinning – Let us begin with the strong pinning case of $\alpha = 0.2$. The equilibrium state is a pinned solid (VG) as random as liquid seen from the structure factor. The $v - F$ characteristics at low temperatures are depicted in Fig. 1 ($T = 0$ in inset). A continuous depinning transition is observed at $T = 0$ with a unique depinning force [24], which can be described by $v \simeq A(F/F_{c0} - 1)^\beta$ with $F_{c0} \simeq 0.231 \pm 0.002$ and $\beta \simeq 0.74 \pm 0.02$. For $0 < T < 0.0005$, upward-convex $v - F$ characteristics are observed down to F_{c0} ; below F_{c0} there is an extremely small tail which is hard to see in the present scale.

The sharp depinning transition is clearly rounded by finite temperatures. In order to explore the critical properties of the $v - F$ characteristics at finite temperatures, we postulate the following scaling ansatz [25, 26, 27]

$$v(T, F) = T^{1/\delta} S(T^{-1/\beta\delta} f) \quad (2)$$

with $f = 1 - F_{c0}/F$ [28] and the scaling function $S(x)$

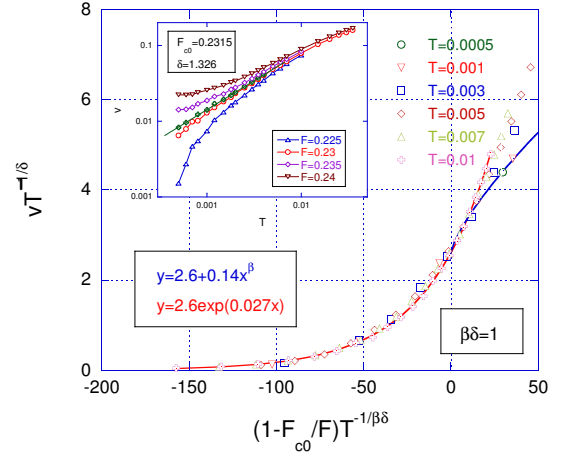


FIG. 2: Scaling plot for the data in Fig.1. Inset: Temperature dependence of velocity for several forces around F_{c0} .

regular at $x = 0$ and $S(x) \rightarrow x^\beta$ as $x \rightarrow +\infty$.

The critical force can be determined using the property $v(T, F = F_{c0}) = S(0)T^{1/\delta}$ implied in Eq. (2) (see also [29]). As shown in the inset of Fig. 2, we evaluate $F_{c0} = 0.2315 \pm 0.0013$, and meanwhile from the slope $1/\delta = 0.754 \pm 0.010$. We then perform the scaling plot using the scaled variables $vT^{-1/\delta}$ and $(1 - F_{c0}/F)T^{-1/\beta\delta}$; the best collapsing of data to a single scaling curve is achieved when $\beta \simeq 1/\delta = 0.754$, thus determining the exponent β . The values of F_{c0} and β estimated from data at finite temperatures via the scaling analysis are consistent with those derived from $T = 0$, which can be taken as an evidence for the existence of scaling. Fitting the scaling curve, we obtain $S(x) = 0.14x^\beta + 2.6$ for $x > 0$ and $S(x) = 2.6\exp(0.027x)$ for $x < 0$; the former covers the continuous depinning transition at $T = 0$; the latter, combined with the relation $\beta\delta = 1$, indicates that the motion at low temperatures and forces below F_{c0} is well described by the Arrhenius law, and that the energy barrier disappears linearly when the force is ramped up to F_{c0} ; the bare energy barrier is $U_c = 0.027$.

The same exponents and similar scaling behaviors are available for $\alpha = 0.4$; therefore, the above properties are universal for strong pinning case. The creep law derived above confirms the *a priori* assumption in the Anderson-Kim theory [30], and coincides with the FRG results in Ref. [31] for a domain wall ($N = 1$). Our results are also consistent with Ref. [29] provided $\theta = 1$.

Deviations from the scaling curve are observed for (a) $F_{c0}/2 < F < F_{c0}$ at $T \geq 0.015 \simeq U_c/2$, due to extra thermal deformation of flux-line lattice; (b) $F < F_{c0}/2$ which may be governed by the zero-force limit; and (c) $F \gg F_{c0}$ the flux-flow regime.

Weak collective pinning – We have performed the same simulations for $\alpha = 0.05$, which falls into the weak collective pinning regime. The equilibrium state is a BrG, with the melting temperature $T_m \simeq 0.077$ above which the quasi long-range order is suppressed by thermal fluctua-

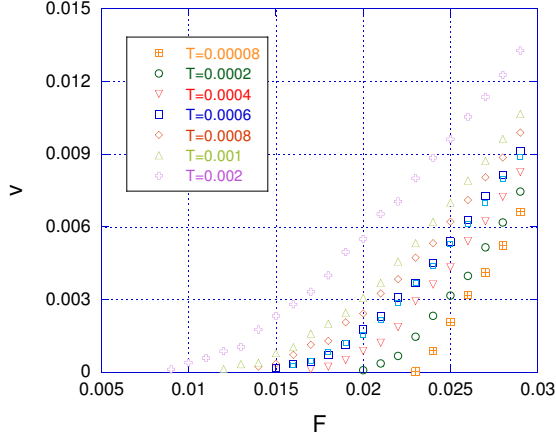


FIG. 3: $v - F$ characteristics for $\alpha = 0.05$. Data for $T = 0.0006$ obtained for $L_{xy} = 40\lambda_{ab}$ are also included (light-blue squares).

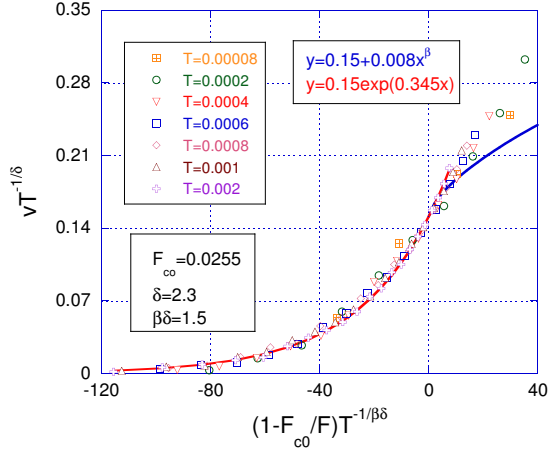


FIG. 4: Scaling plot for data in Fig. 3.

tions. Looking at the velocity-velocity correlation function, we find in this case that the moving system shows good temporal and spatial orders characterized by Bragg peaks [32, 33] (No moving smectic [34] was observed for the present parameters.) The $v - F$ characteristics are shown in Fig. 3, where similar to the strong pinning case, a sharp crossover between the depinning and creep motion takes place at F_{c0} for $0 < T \leq 0.00008$. The scaling plot is depicted in Fig. 4. The exponents are estimated as $\delta = 2.3 \pm 0.1$ and $\beta = 0.65 \pm 0.01$, which are different from those for strong pinning case. The product of the two exponents $\beta\delta = 3/2$ deviates from unity, indicating a nonlinear scaling relation between temperature and force deviation from F_{c0} .

Nonlinear scaling relations have been found in CDW systems [26]. This behavior can be captured by an effective potential of linear and cubic terms of displacement, with a small energy barrier [12, 26]. The linear scaling relation observed for strong pinning force corresponds to an

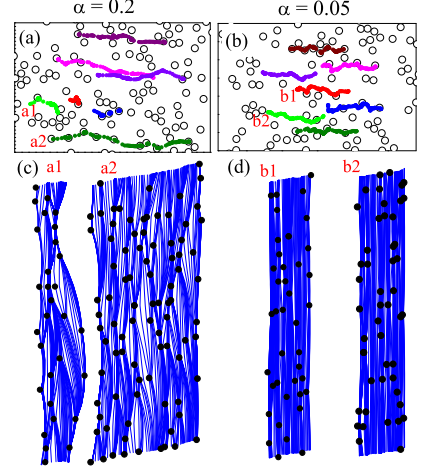


FIG. 5: Vortex motions at $T = 0$. (a) and (b): Trajectories of 7 nearest-neighboring vortices on one layer for $\alpha = 0.2$ at $F = 0.24$ and $\alpha = 0.05$ at $F = 0.027$ respectively. (c) and (d): Trajectories of the two flux lines indicated in (a) and (b). The total times are 330 for $\alpha = 0.2$, and 1200 for $\alpha = 0.05$, such that flux lines in both systems move roughly the same distance $4\lambda \sim 1.7a_0$ in average. Open circles in (a) and (b) represent the positions of pins, while the filled circles in (c) and (d) represent pins that pin the flux lines.

effective potential of linear, quadratic and quartic terms of displacement, with a large energy barrier [35]. It is observed in our simulations that the system with weak bare pinning strength experiences smaller energy barriers compared with that of strong bare pinning strength, even at the *same* relative force-deviation from the critical values; an analytic derivation of the effective energy barrier, however, is not an easy task [12]. While a full picture remains to be developed, we notice that, first, vortex motions mimic nucleation processes in first-order phase transitions: the weak/strong pinning case corresponds to a system locates at the spinodal/coexistence curve [35]; secondly, under weak and strong pinning vortices behave similarly to CDW [26] and domain wall [31] respectively, due to the different ranges of correlation.

The scaling curve in Fig. 4 is fitted well by $S(x) = 0.15 \exp(0.0345x)$, which, with the nonlinear scaling variable, indicates a non-Arrhenius creep motion for the weak pinning case. To the best of our knowledge, this behavior has not been reported so far. On a phenomenological level, it can be captured with an appropriate correlator of energy barriers [36].

"Microscopic" vortex motion— We have examined the *microscopic* motions of flux lines. As detailed in Fig. 5 for forces slightly above F_{c0} and at zero temperature (similar results have been obtained for $F < F_{c0}$ at finite temperatures), flux lines in the weak pinning case move homogeneously in an intermediate time scale, which guarantees the moving BrG (mBrG) order [33]; flux lines under strong pinning move in an inhomogeneous way, and thus additional dislocations are induced during the motion.

Even for the case of mBrG, velocity fluctuates for time being and between different vortices, as can be seen in Fig. 5d. Namely in a shorter time scale, the motion of vortices in weak pinning case is also random: Flux lines exhibit an intermittent pattern of motion, *i.e.* a portion of flux lines move while others are almost motionless at a given time window, and in the next time window, similar situation occurs with the moving vortices found in different regions. The motion of the total system is thus an accumulation of individual, random movements, in which creep events dominate and the random pinning plays an essential role. As shown in Figs. 5c and d the shape of vortex lines upon depinning depends on pin strength [23].

Discussions—The strong pinning $\alpha = 0.2$ and weak collective pinning $\alpha = 0.05$ according to the Labusch criterion [22, 23] result in vortex glass and Bragg glass respectively. But generally the Labusch criterion does not coincide with the phase boundary of Bragg glass. Further study is expected to resolve this point in detail.

As can be seen in Figs. 5a and b, during the creep motion vortices displace frequently into the direction transverse to the force and the averaged velocity. In this way a bypath of lower energy can be found which assists vortices to avoid otherwise high energy barriers. This

may affect the averaged velocity significantly since the time spent in large energy barriers is huge, and is to be taken into account carefully in theoretical treatments.

Beside the genuine, zero-temperature depinning transition, we observe a quite steep crossover between the depinning and creep motions at low temperatures ($T \leq 0.0005$ for $\alpha = 0.2$ and $T \leq 0.00008$ for $\alpha = 0.05$). The velocity tail below the crossover is very small as such it looked like a phase transition in simulations (and perhaps also in experiments). The crossover, however, loses its sharpness when temperature increases but still far below the melting temperature, which might be not quite consistent with experimental phase boundary $H_g(T)$ [14]. The possibility of a transition (or sharp crossover) between the depinning and flux flow regimes remains to be investigated within the present formalism, taking into account the shaking magnetic field.

Acknowledgements – We are pleased to acknowledge T. Nattermann, D. Genshkenbein, G. Blatter, B. Rosenstein, V. Vinokour and D. P. Li for discussions. Calculations were performed on SR11000 (HITACHI) in NIMS. X. H. is supported by Grant-in-Aid for Scientific Research (C) No. 18540360 of JSPS, and project ITSNEM of China Academy of Science.

-
- [1] T. Nattermann, Phys. Rev. Lett. **64**, 2454 (1990).
 - [2] T. Giamarchi and P. Le Doussal, Phys. Rev. Lett. **72**, 1530 (1994); Phys. Rev. B **52**, 242 (1995).
 - [3] D. S. Fisher, M. P. A. Fisher and D. A. Huse, Phys. Rev. B **43**, 130 (1991).
 - [4] A. I. Larkin and Yu. N. Ovchinnikov, J. Low Temp. Phys. **34**, 409 (1979).
 - [5] L. B. Ioffe and V. M. Vinokur, J. Phys. C **20**, 6149 (1987).
 - [6] T. Nattermann, EuroPhys. Lett. **4**, 1241 (1987).
 - [7] M. V. Feigel'man *et al.*, Phys. Rev. Lett. **63**, 2303 (1989).
 - [8] G. Blatter *et al.*, Rev. Mod. Phys. **66**, 1125 (1994);
 - [9] P. Chauve, T. Giamarchi, P. Le Doussal, Phys. Rev. B **62**, 6241 (2000).
 - [10] T. Giamarchi and S. Bhattacharya, *High Magnetic Fields: Applications in Condensed Matter Physics, Spectroscopy* (Springer, New York, 2002), p.314.
 - [11] T. Nattermann and S. Scheidl, Adv. Phys. **49**, 607 (2000).
 - [12] S. Brazovskii and T. Nattermann, Adv. Phys. **53**, 177 (2004).
 - [13] A. B. Kolton, A. Rosso and T. Giamarchi, Phys. Rev. Lett. **94**, 047002 (2005).
 - [14] H. Beidenkopf *et al.*, Phys. Rev. Lett. **95**, 257004 (2005).
 - [15] D. P. Li and B. Rosenstein, cond-mat/0411096.
 - [16] S. Ryu *et al.*, Phys. Rev. Lett. **68**, 710 (1992).
 - [17] C. Reichhardt, C. J. Olson and F. Nori, Phys. Rev. Lett. **78**, 2648 (1996).
 - [18] A. van Otterlo, R. T. Scalettar, and G. T. Zimányi, Phys. Rev. Lett. **81**, 1497 (1998).
 - [19] E. Olive *et al.*, Phys. Rev. Lett. **91**, 37005 (2003).
 - [20] Q. H. Chen and X. Hu, Phys. Rev. Lett. **90**, 117005 (2003); The work clarifies the regime of current and temperature where vortex loops are excited, which is beyond the application of the present model.
 - [21] E. Zeldov *et al.*, Nature **375**, 373 (1995).
 - [22] R. Labusch, Cryst. Lattice Defects, **1**, 1 (1969).
 - [23] G. Blatter, V. B. Geshkenbein and J. A. G. Koopmann, Phys. Rev. Lett. **92**, 67009 (2004).
 - [24] A. Alan. Middleton, Phys. Rev. Lett. **68**, 670 (1992). The theory works for the present case but cannot be proved explicitly.
 - [25] D. S. Fisher, Phys. Rev. Lett. **50**, 1486 (1983); *ibid* Phys. Rev. B **31**, 1396 (1985).
 - [26] A. Alan. Middleton, Phys. Rev. B **45**, 9465 (1992).
 - [27] L. Roters *et al.*, Phys. Rev. B **60**, 5202 (1999).
 - [28] The usually adopted quantity $f' = 1 - F/F_{c0}$ gives the same exponents, but the scaling regime is much narrower.
 - [29] T. Nattermann, V. Pokrovsky, and V. M. Vinokur, Phys. Rev. Lett. **87**, 197005 (2001).
 - [30] P. W. Anderson and Y. B. Kim, Rev. Mod. Phys. **36**, 39 (1964).
 - [31] M. Müller, D. A. Gorokhov, G. Blatter, Phys. Rev. B **63**, 184305 (2001).
 - [32] L. Balents and M. P. A. Fisher, Phys. Rev. Lett. **75**, 4270 (1995).
 - [33] T. Giamarchi and P. Le Doussal, Phys. Rev. Lett. **76**, 3408 (1996); P. Le Doussal and T. Giamarchi, Phys. Rev. B **57**, 11356 (1998).
 - [34] L. Balents, M. Cristina, and L. Radzihovsky, Phys. Rev. Lett. **78**, 751 (1997); *ibid* Phys. Rev. B **57**, 7705 (1998).
 - [35] Y. Sang, M. Dubé, and M. Grant, Phys. Rev. Lett. **87**, 174301 (2001).
 - [36] P. Le Doussal and V. M. Vinokur, Physica C, **254**, 63 (1995).